

## Generation, transport, and trapping of excess charge carriers in Czochralski-grown sapphire

R. C. Hughes

*Sandia Laboratories,\* Albuquerque, New Mexico 87185*

(Received 21 December 1978)

The transient x-ray-induced conductivity in high-purity Union Carbide  $\text{Al}_2\text{O}_3$  single crystals is reported. The mobility lifetime product for electrons is much greater than that for holes and consequently the transport properties of the holes remain obscured. The trapping and detrapping rates for four different electron traps were determined from the data, including the trapping parameters for substitutional  $\text{Cr}^{3+}$ . Even though the transport is dominated by trapping and detrapping, the high-mobility transport of electrons was observed in the first few nanoseconds; the mobility was found to be  $3 \pm 1 \text{ cm}^2/\text{Vsec}$  independent of temperature between 100 and 350 K. The magnitude and temperature dependence of the intrinsic mobility are not in agreement with simple large-polaron theory. It was found that one of the deep traps (not  $\text{Cr}^{3+}$ ) could be filled with an accumulated dose of 2000 rad at 300 K, and that the filling led to an increase of up to fivefold in the lifetime.

### I. INTRODUCTION

"Sapphire" is now a common usage term for very pure single crystal  $\alpha\text{-Al}_2\text{O}_3$  which is finding widespread technological uses as an electrical insulator (in silicon-on-sapphire microcircuits, for example) and as an optical material. There have been many investigations<sup>1,2</sup> of radiation damage to sapphire, including optical and ESR studies of the color centers and transient measurements of thermoluminescence and thermally stimulated currents. Radiation damage caused by low linear energy transfer (LET) ionizing radiation, like x-rays and electrons, is largely due to the diffusion of thermal electrons and holes to defects and impurities in the lattice. The purpose of the work presented here is to describe the behavior of excess electrons and holes in a wide time frame ( $10^{-9}$ – $10^{+3}$  sec) after they have been created by ionizing radiation. Even though the carrier transport is dominated by trapping at defects and impurities, the behavior of free carriers is observed in the first few nanoseconds. I have been able to characterize at least four different electron traps in this type of sapphire, including the role of the famous  $\text{Cr}^{3+}$  substitutional impurity (ruby).<sup>2</sup> The photocurrent behavior is complicated by multiple trapping, which upon analysis gives the trapping and detrapping rates for the four traps. However, there is no "dispersive" transport as in pure amorphous  $\text{SiO}_2$ . In Sec. III, the conductivity as a function of time and temperature is presented, as well as time-of-flight experiments for the charge carriers. Modifications of the trapping behavior by adding various amounts of  $\text{Cr}^{3+}$  and filling of the traps by carriers are described. In Sec. IV the analysis of the conductivity data in terms of

trapping and detrapping rates is given. There is also a comparison of behavior of excess carriers in sapphire with crystalline and amorphous  $\text{SiO}_2$ .

### II. EXPERIMENTAL

The sapphire reported on here is Union Carbide, Czochralski grown, uv grade. This type of high-purity sapphire has been developed in response to the needs of the integrated circuit industry, where silicon-on-sapphire technology is becoming increasingly important. Impurity concentrations have been catalogued for this kind of sapphire, and the  $\text{Cr}^{3+}$  and  $\text{Fe}^{3+}$  impurities are found to be in the few ppm range or less.<sup>3</sup> Other defects have been discussed by Crawford and his co-workers.<sup>1,2</sup> Disks of thicknesses ranging from 250 to  $10^3 \mu\text{m}$  and three orientations relative to the  $c$  axis ( $0^\circ$ ,  $45^\circ$ , and  $90^\circ$ ) were purchased. Evaporated Al electrodes were used to make plane-parallel capacitor samples. The samples were mounted in a vacuum chamber or potted in epoxy to avoid photocurrent signals due to air ions. The experimental details have been given elsewhere<sup>4,5</sup>; the excitation of electron-hole pairs in the sapphire is by a 3-nsec-wide x-ray pulse from a Febetron 706.

Changes in experimental technique for these results include data acquisition by a Tektronix 7912 Transient Digitizer which allows digitizing of the data in the nanosecond range and subsequent normalization to dose received and other manipulations. In the experiments to determine the sign of the charge carrier with the largest mobility-lifetime product, a platinum foil was placed in intimate contact with one Al electrode. The high-Z Pt receives a much higher dose from the same flux of x rays as the sapphire or evaporated Al layer and because of electron equilibrium considerations,

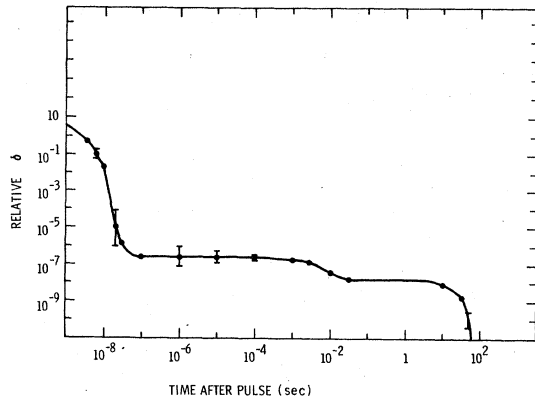


FIG. 1. Log-log plot of the relative conductivity vs time for a typical sapphire sample at 300 °K. The applied field and the number of excess carriers are kept low enough so that all conductivity decays depicted are due to first-order trapping kinetics. The excitation pulse is  $3 \times 10^{-9}$  sec wide. The error bars reflect the experimental error in taking the derivative of charge collection data in the given time ranges.

the layer of sapphire next to the Pt develops a higher density of electron-hole pairs than in the bulk of the sample.<sup>6</sup> The shape of the x-ray spectrum from the Febetron 706 is not known accurately, so even though computer codes are available for calculating the dose near interfaces, only a crude estimate was made for the dose distribution in the sapphire under the asymmetric conditions. The data identifying the negative carrier as the major contributor were fairly unambiguous, even though the relative mobility-lifetime product for the negative and positive carriers were not determined.

The  $\text{Cr}^{3+}$  doped samples (i.e., ruby) were also produced by Union Carbide in the same fashion as the "pure" sapphire. In the trap-filling experiments the high doses were administered to the samples by a GE x-ray machine operating at 60 kV.

### III. RESULTS

#### A. Transient conductivity

High-energy x rays produce a nearly uniform distribution of electrons and holes in the bulk of the sapphire crystal. The excess conductivity of these carriers can be measured by their displacement current in an applied field. Figure 1 gives the conductivity over many orders of magnitude under conditions which guarantee that no significant number of carriers is lost by bulk recombination or sweeping out to the electrodes, and that there are no space charge induced distortions in the photocurrent profiles. The decay in the conductivity is then caused solely by first-order trapping kinetics. There are four distinct regions in the conductivity curve: (i) a prompt, high-mobility component which decays exponentially with a time constant of a few nanoseconds over several orders of magnitude, (ii) and (iii) there are two plateaus in the conductivity with the higher one decaying into the lower with a time constant of about  $2 \times 10^{-3}$  sec, and (iv) the conductivity decays, again exponentially, to levels below our detectability with a time constant of a few seconds, at room temperature.

The data are suggestive of trap modulation of the carrier mobility in which there are at least three

TABLE I. Lifetime  $\tau_3$  and mobility data for nine sapphire samples. The cut refers to the angle of the normal to the sample disk to the  $c$  axis of the crystal. The  $\mu_{\text{eff}}$  is derived from transit-time data.

Sample	"Cut"	$\tau_3$ at 270 °C (sec)	$\mu_{\text{eff}}$ at 270 °C	$\mu_{\text{eff}}\tau_3$ ( $\text{cm}^2/\text{V}$ )
1	0°	3.3	$2.8 \times 10^{-8}$	$9.2 \times 10^{-8}$
2	0°	4.4	$2.3 \times 10^{-8}$	$1.01 \times 10^{-7}$
3	0°	2.8	$3 \times 10^{-8}$	$8.4 \times 10^{-8}$
3	0°	8.5 <sup>a</sup>	$3 \times 10^{-8}$	$2.6 \times 10^{-7}$
4	45°	3.7	$3 \times 10^{-8}$	$1.1 \times 10^{-7}$
4	45°	10	$3 \times 10^{-8}$	$3 \times 10^{-7}$
5	45°	5.7	$2.1 \times 10^{-8}$	$1.2 \times 10^{-7}$
6	45°	4.4	$2.1 \times 10^{-8}$	$9.3 \times 10^{-8}$
6	45°	12.5 <sup>a</sup>	$2.3 \times 10^{-8}$	$2.6 \times 10^{-7}$
6	45°	2.1 <sup>b</sup>		
7	45°	3.8	$1.8 \times 10^{-8}$	
7	45°	22s <sup>a</sup>		
8	90°	4.8	$1.6 \times 10^{-8}$	$7.7 \times 10^{-8}$
9	90°	6.2	$1.4 \times 10^{-8}$	$9 \times 10^{-8}$
9	90°	20 <sup>a</sup>	$1.4 \times 10^{-8}$	$2.8 \times 10^{-7}$

<sup>a</sup> 3000 rad accumulated dose.

<sup>b</sup> 500 °K anneal after high accumulated dose.

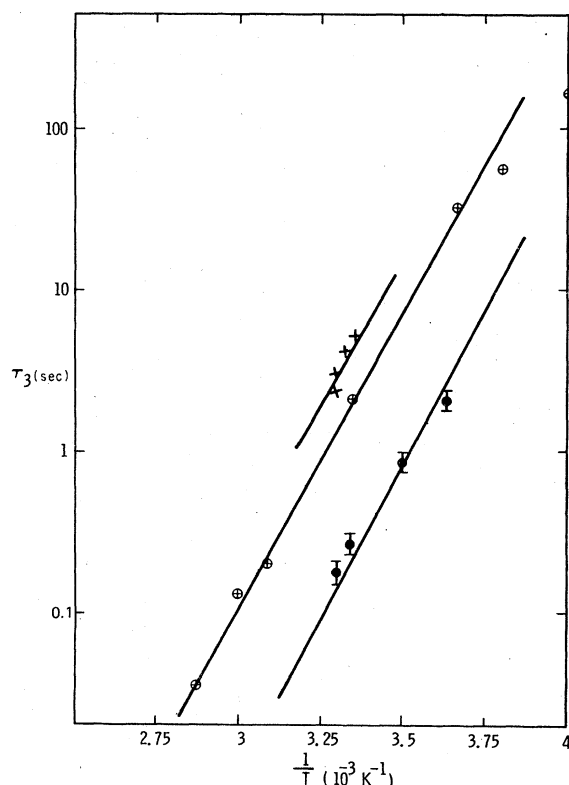


FIG. 2. Long lifetime  $\tau_3$  as a function of temperature for three samples. The shortest lifetime curve is for a sample doped with  $6 \times 10^{18} \text{ Cr}^{3+}$ . The other two are nominally pure sapphire.

traps. Two of the traps have release rates greater than  $1 \text{ sec}^{-1}$ , which create the two plateaus. The release rate of the third is too low to be detected at room temperature, but may be observed in higher-temperature thermally stimulated current (TSC) experiments and/or thermally stimulated luminescence (TSL) experiments. Table I gives the values for the long-term lifetime ( $\tau_3$ ) in the samples that were investigated.

#### B. Temperature dependence of the conductivity

The prompt part of the conductivity is only very weakly temperature dependent, while the other portions are very strongly temperature dependent. Figure 2 gives  $\tau_3$  as a function of temperature for three different samples; the longer lifetime samples are nominally "pure" and the lower is a  $\text{Cr}^{3+}$  doped sample. The presence of the same activation energy, 0.75 eV, for the different samples indicates that the activation energy is found in the release rate  $q_2$ , which is independent of the number of deep traps controlling  $\tau_3$ .

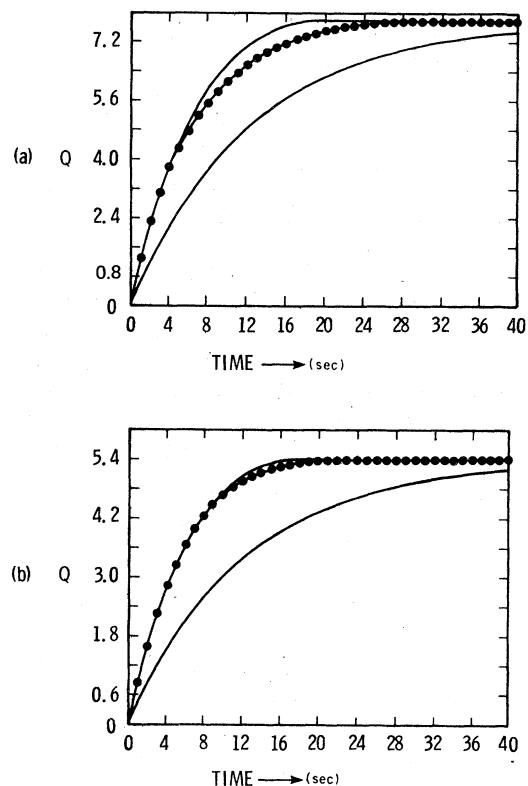


FIG. 3. Integrated photocurrent at  $10^5 \text{ V/cm}$  in the regime where sweepout of the carriers dominates the carrier lifetime. The curve designated by the circles is the data points. The lower curve is taken from data at much lower fields where the bulk lifetime of the carriers dominates the photocurrent. The upper solid line is a fit to the data employing the measured lifetime and the best-fit sweepout time. The experimental setup is described in the text, but this data show the special case where the concentration of electron-hole pairs was not uniform throughout the bulk of the sample, but was enhanced near one electrode by a layer of high- $Z$  metal. Curve (a) was for a negative polarity at the high-density electrode, and curve (b) was for a positive polarity. Each curve was normalized to the same x-ray flux.

#### C. Yield of electron-hole pairs

The number of electron-hole pairs produced by a given dose of radiation ( $\text{rad} = 100 \text{ ergs/g}$ ) is of interest because it is much less than expected from the band-gap energy (about 9 eV in sapphire). For low applied fields the energy required is  $75 \pm 7 \text{ eV}/(\text{electron-hole pair})$ , which can be compared to  $150 \text{ eV}/(\text{electron-hole pair})$  for amorphous  $\text{SiO}_2$ .<sup>7</sup> The yield is weakly field dependent, as expected for geminate recombination, but no data were taken above  $10^5 \text{ V/cm}$ , where I would expect the yield to increase to the vicinity of  $20 \text{ eV}/(\text{electron-hole pair})$ , as it does in  $\text{SiO}_2$ .<sup>7</sup> The

higher dielectric constant in  $\text{Al}_2\text{O}_3$  over  $\text{SiO}_2$  can account for the increased yield.

#### D. Carrier "mobility"

The deep trapping lifetime  $\tau_3$  is long enough so that a significant fraction of the carriers can be swept from the bulk of the sample to the electrodes. The effective carrier mobility may be determined from the field and thickness dependence of the conductivity curves like Fig. 1. Experimentally, only the shape of the final decay is affected at the fields and thickness employed. For experimental reasons, the integral of the photocurrent is measured and the effective mobility is obtained by fitting the data to the expression<sup>8</sup>

$$Q(t) = \left( N_0 e \mu_{\text{eff}} \frac{V}{d} \right) \left\{ \left[ \left( \frac{\tau}{t_s} \right) t + \tau \left( \frac{\tau}{t_s} - 1 \right) \right] e^{-t/\tau} - \tau \left( \frac{\tau}{t_s} - 1 \right) \right\}, \quad (1)$$

where  $t_s$  is the sweepout time, which is  $t_s = d^2 / \mu_{\text{eff}} V$ , where  $d$  is the sample thickness,  $V$  is the applied voltage, and  $N_0$  is the bulk concentration of carriers. The  $\mu_{\text{eff}}$  obtained from these fits for the different samples are given in Table I for 26°C. It turns out that the effective mobilities are activated with the same activation energy as  $\tau_3$ , which means that the mobility-lifetime product is independent of temperature within experimental error. It can be seen from Fig. 1 that this very low mobility is not the "free" carrier mobility, but is dominated by the release time from traps, a trap-modulated mobility.

When electron-hole pairs are created uniformly in the bulk of the sample it is not possible to tell from the photocurrent which sign of carrier is dominating the photocurrent. The detection of more than one rate of decay as in Fig. 1 *might* indicate the different fates of the positive and negative carriers, but cannot predict which is which. I obtained a qualitative indication that the negative carrier dominates the transport by introducing an asymmetry in the concentration of electron-hole pairs in the sample. This was accomplished by placing a high- $Z$  material behind the back electrode of the sample, which enhances the dose close to that side of the sample. Figure 3 displays the effect of this asymmetry on the shape and magnitude of the integrated photocurrent. In (a) the high dose electrode was biased negatively so that excess electrons would be pushed towards opposite electrode. In (b) the high dose electrode was biased positively. The larger integrated charge in (a) indicates that more charge is being carried by the negative carrier, or more precisely, that the mo-

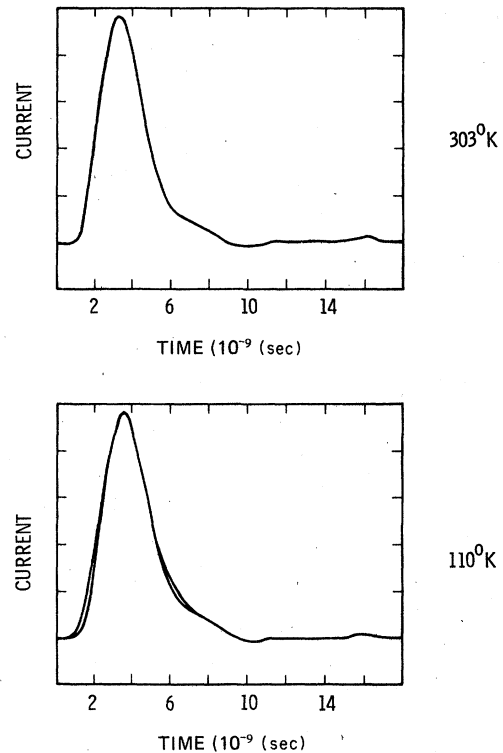


FIG. 4. Prompt current at two different temperatures, 303 and 110 °K. The shape of the pulse is dominated by the x-ray pulse, but from the small tail the prompt trapping lifetime can be estimated to be about  $2 \times 10^{-9}$  sec. The lifetime is not noticeably temperature dependent, but the photocurrent at the same dose and field is down by a factor of 0.75 at 110 °K. The curve designated by the triangles in the 110 °K data is taken at  $10^5$  V/cm, while the other curve was taken at  $4 \times 10^4$  V/cm. The peak amplitude of the currents have been normalized to facilitate inspection of the effect of field on the lifetime.

bility-lifetime product for electrons is greater than that for holes.

The high current or "prompt" portion of the conductivity is displayed in more detail in Fig. 4. The carrier lifetime (most likely electrons) obtained from this data is not as accurate as those obtained for single-crystal and amorphous  $\text{SiO}_2$  because the lifetime is not long compared to the width of the x-ray pulse. However, comparison of the photocurrents in Fig. 4 with those from a  $p$ - $i$ - $n$  diode (where the sweepout time of the carriers is much shorter than  $10^{-9}$  sec) indicates that the carrier lifetime is about  $2 \times 10^{-9}$  sec. One crystal (S-2) showed a 4-nsec lifetime, and an attempt was made to induce carrier sweepout in that sample at very high voltages (up to 30 kV across 300  $\mu\text{m}$ ) by the method discussed in Ref. 9. Only a weak indication of sweepout behavior could be found, showing that the mobility is less than  $10 \text{ cm}^2/\text{V sec}$ . The prompt mobility can be better determined by using

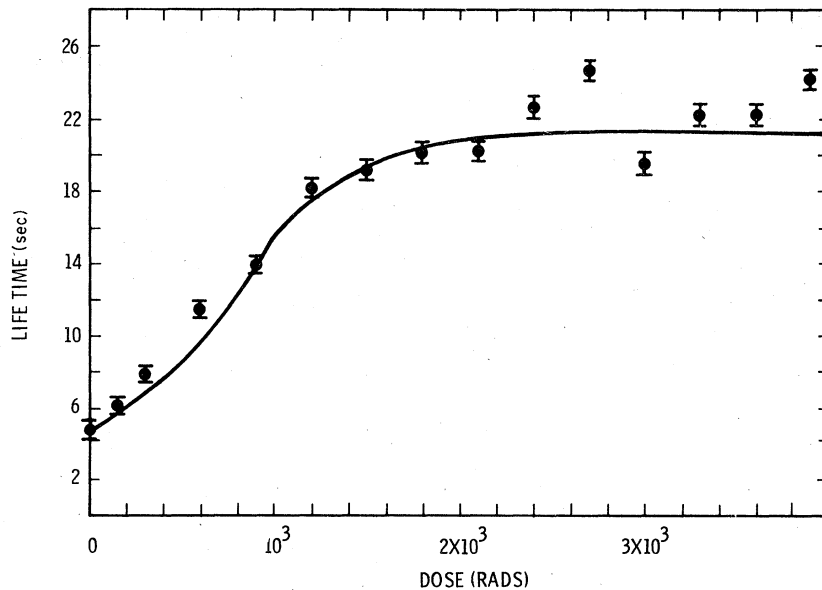


FIG. 5. Lifetime  $\tau_3$  in sample 7 as a function of the accumulated dose at 300 K. The curve is from the theory in the text.

the long-term sweepout to define the number of electrons undergoing transport in the crystal after the pulse (from the mobility-lifetime product). The ratio of the mobility-lifetime products for the prompt portion and the delayed portion, along with the prompt lifetime give the prompt mobility  $\mu_p$  with no adjustable parameters and no need to know the dose delivered to the sample. Averaged over several samples it was found to be  $3 \pm 1$  cm<sup>2</sup>/V sec, which is consistent with the sweepout data mentioned above.

It can be noted from Fig. 4 that there is almost no temperature dependence to the prompt portion; the lifetime stays the same and the number of carriers per unit dose is 0.75 of room temperature. The delayed portions, as is expected from the high activation energy, are not detectable at 110°K.

#### E. Trap filling experiments

I have found that  $\tau_3$  varies somewhat from sample to sample even from the same boule, as shown in Table I. Much larger variations can be produced by accumulating a moderate x-ray dose in a given sample. An example of this is given in Fig. 5, where the sample was exposed in a shorted condition to a given x-ray dose and the new lifetime measured. The pulsed lifetime measurements were carried out with doses of about 0.1 rad, so that the lifetime is not measurably changed during the pulsing. From the yield measurements, I know that 1800 rad of accumulated dose have produced about  $5 \times 10^{15}$  (electron-hole pairs)/cm<sup>3</sup>. Because of the fast trapping rates and the low dose rate employed, very few of these electron-hole pairs will undergo bulk recombination; therefore, they all

end up in some trap with first-order kinetics. The shorter lifetime can be restored to a sample by annealing it at above 500°K for a few hours. The heavily doped Cr<sup>3+</sup> samples ( $10^{18}$  Cr<sup>3+</sup>/cm<sup>3</sup>) showed no change in  $\tau_3$  when given the same accumulated dose.

#### F. Cr<sup>3+</sup>-doped samples

In addition to the nominally pure sapphire samples, three Cr<sup>3+</sup> doped samples were characterized. The effect of Cr<sup>3+</sup> concentration on the lifetime  $\tau_3$  is shown in Fig. 6.

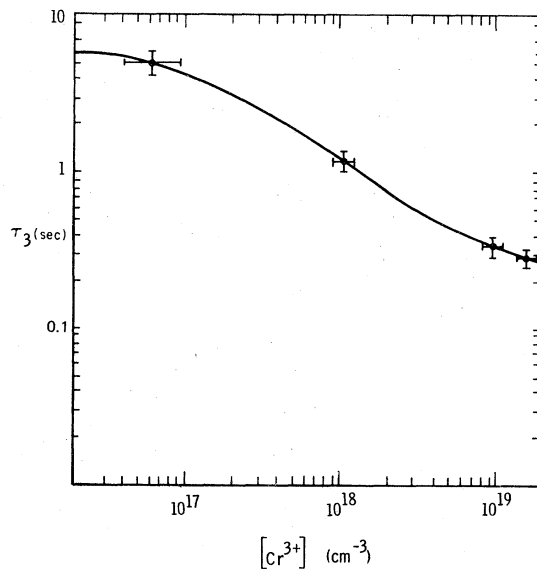


FIG. 6. Lifetime  $\tau_3$  as a function of the concentration of substitutional Cr<sup>3+</sup>.

## IV. DISCUSSION

## A. Trapping kinetics

The transport data presented in the previous section can be described with a model which has four different kinds of electron traps, with trapping rates which depend in the usual fashion on concentration, and release rates which also depend in the usual fashion (Arrhenius) on temperature. The presence of two plateaus and well-defined exponential decays between plateaus tell us that only two of the four release rates are significant at room temperature and that they are many orders of magnitude slower than the trapping rates. The predicted current versus time curves can be generated by numerical computer solutions for any number of trapping and release rates, as shown by the simulations of the dispersive transport in  $\alpha$ -SiO<sub>2</sub>, where the variety of events is so great that the individual plateaus and decays cannot be separated from one another experimentally. However, in this case I feel it is informative to give the analytical solution for two traps and two release rates and proceed to the simple approximations which allow the rates to be extracted from the data.

The trapping rate for each trap will be designated by  $k_n$  and the release rate by  $q_n$ . The differential equations to be solved are

$$\frac{dn_f}{dt} = -(k_1 + k_2)n_f + q_1n_1 + q_2n_2, \quad (2)$$

$$\frac{dn_1}{dt} = k_1n_f - q_1n_1, \quad (3)$$

$$\frac{dn_2}{dt} = k_2n_f - q_2n_2, \quad (4)$$

where  $n_f$  is the concentration of free carriers, and  $n_1$  and  $n_2$  are the population of the respective traps. In this solution it is assumed that the trapping rate  $k_n$  is not affected by the occupation of the trap, i.e., the total number of carriers introduced by the excitation pulse,  $n_0 = n_f + n_1 + n_2$ , is much smaller than the concentration of traps. In the trapping experiments described below, this assumption will be removed.

As expected, the solution of these differential equations for  $n_f(t)$ , which is always proportional to the measured conductivity, is a sum of two exponentials with a final conductivity plateau (i.e., steady state) given by

$$\frac{n_f(\infty)}{n_0} = \frac{q_1q_2}{C}, \quad (5)$$

where  $C = k_1q_2 + k_2q_1 + q_1q_2$ . The corresponding steady-state populations of the traps are given by

$$\frac{n_1(\infty)}{n_0} = \frac{k_1q_2}{C} \quad (6)$$

and

$$\frac{n_2(\infty)}{n_0} = \frac{k_2q_1}{C}. \quad (7)$$

The time-dependent concentration of the traps is

$$n_1(t) - n_1(\infty) = C_1e^{-\lambda_-t} - C_2e^{-\lambda_+t}, \quad (8)$$

$$n_2(t) - n_2(\infty) = -d_1e^{-\lambda_-t} - d_2e^{-\lambda_+t}, \quad (9)$$

where the decay rates are given by

$$\lambda_{\pm} = \frac{1}{2} [B \pm (B^2 - 4C)^{1/2}], \quad B = k_1 + k_2 + q_1 + q_2. \quad (10)$$

The constants are given by

$$C_1 = [k_1n_0/(\lambda_+ - \lambda_-)C](C - q_2\lambda_+), \quad (11)$$

$$C_2 = [k_1n_0/(\lambda_+ - \lambda_-)C](C - q_2\lambda_-), \quad (12)$$

$$d_1 = [k_2n_0/(\lambda_+ - \lambda_-)C](q_1\lambda_+ - C), \quad (13)$$

$$d_2 = [k_2n_0/(\lambda_+ - \lambda_-)C](C - q_1\lambda_-). \quad (14)$$

Some simple approximations result immediately from the fact that  $k_1, k_2 \gg q_1, q_2$ :

(i) The "prompt" decay is just  $B = k_1 + k_2 \sim \lambda_+$ .

(ii) The intermediate decay, which is mostly a reequilibration of trap populations from the trap with the fast release rate ( $q_1$ ) to the one with the slow release rate ( $q_2$ ), is

$$\lambda_- = C/B. \quad (10a)$$

(iii) The ratio of free carriers to trapped in the first (higher) plateau is then

$$\frac{n_f}{n_0} \cong \frac{q_1 + q_2 - C/B}{B}, \quad (15)$$

which is proportional to the conductivity.

The four rate constants can now be readily extracted from the known experimental data (ignoring the final decay,  $1/\tau_3 = k_3 + k_4$ , which is much slower):

(i)  $B = k_1 + k_2 \cong 5 \times 10^8 \text{ sec}^{-1}$  from the prompt decay;

(ii)  $\lambda_- \cong C/B \cong 500$ ,  $C = 2.5 \times 10^{11} \text{ sec}^{-2}$ ;

(iii)  $n_f(\infty)/n_0 = q_1q_2/C$ , so  $q_1q_2 = 2.5 \times 10^3 \text{ sec}^{-2}$ ,

which confirms the assumption that  $k_1, k_2 \gg q_1, q_2$ .

(iv) Then the individual rates  $q_1$  and  $q_2$  come from Eq. (15),  $n_f/n_0 \sim 10^{-7}$  and are  $q_1 = 543 \text{ sec}^{-1}$ ,  $q_2 = 4.6 \text{ sec}^{-1}$ .

(v) And from  $C = 2.5 \times 10^{11}$ ,

$$k_2 = 4.6 \times 10^8 \text{ sec}^{-1} \text{ and } k_1 = 4 \times 10^7 \text{ sec}^{-1}.$$

It is seen that trap "1" receives only 7% of the carriers and only contributes a measurable amount to the current because of its fast release rate. It has occurred to me that the excess current caused by trap "1" might actually be due to the motion of

holes, which would not be coupled to the electron trapping and detrapping rates. It will be difficult to prove this one way or the other, since the rate constants can be juggled to fit either case equally well. Surface excitation of electron-hole pairs by low-energy electrons or vacuum ultraviolet light can potentially distinguish the motion of the electron from that of the hole. However, the intermediate current accounts for less than 1% of the total charge measured and thus even if it is due to holes it will be very hard to distinguish experimentally from the electron signal due to finite depth of absorption and other experimental uncertainties (the proof that *most* of the measured current is due to electrons has been given in the results sections from our own asymmetric dose experiments).

Another piece of evidence which indicates that the intermediate current is electrons and not holes is that in the experiments with the  $\text{Cr}^{3+}$  doped samples, the intermediate current is diminished along with the prompt and delayed currents, which is consistent with increasing the magnitude of  $B$ , or sum of the electron trapping rates. Of course, the  $\text{Cr}^{3+}$  may be a hole trap as well as (as has been established) an electron trap, which would again allow the possibility that the intermediate current is due to hole motion.

In the subsequent discussion, the effects of trap "1" will be ignored for simplicity; only a slight adjustment of the rate constants would be necessary to include it. Now the deep trapping lifetime, which has been called  $\tau_3$ , becomes  $B/C$ , which simplifies to

$$\tau_3 \cong (k_2 + k_3 + k_4) / [q_2(k_3 + k_4)] \text{ sec}, \quad (10b)$$

where  $k_3$  refers to the deep traps ( $q_3 = 0$ ) of unknown structure and  $k_4$  refers to the  $\text{Cr}^{3+}$  deep electron trap ( $q_4 = 0$ ); it should be noted that  $\tau_3$  does not just depend on the rate constants for trap-

ping into the deep traps ( $k_3 + k_4$ ), but has a crucial dependence on  $q_2$  which will show up below in the  $\text{Cr}^{3+}$  concentration dependence of  $\tau_3$ .

Another useful approximation is to find the ratio of the total collected charge at small applied fields [see Eq. (1)] for the delayed portion to the prompt portion (an experimental quantity which is fairly easy to measure for a given sample). This quantity turns out to be  $k_2/(k_3 + k_4)$ . For example, in sample 1  $\tau_3$  is 3.5 sec at 26°C, and the ratio of the prompt to the delayed is 1:15. Then  $q_2 = 4.6 \text{ sec}^{-1}$ , as determined in the other analysis. The parameters which fit the data for sample 1 are given in Table II.

## B. Carrier mobility

### 1. "Intrinsic" mobility

The "intrinsic" mobility of an electron or hole in defect-free  $\text{Al}_2\text{O}_3$  will be dominated by electron-phonon interactions. The computation of the mobility in a crystal-like sapphire, where the electron-phonon interaction is relatively large, has presented special difficulties for solid-state theorists.<sup>10,11</sup> The field is quite active with much recent effort expended in understanding the electron mobility in  $\text{SiO}_2$ .<sup>12</sup> In spite of the differences in structure, the important optical phonons in  $\text{Al}_2\text{O}_3$  and  $\text{SiO}_2$  are very similar, probably because Al-O bonds and Si-O bonds are similar.<sup>13</sup> The various theoretical approaches to calculating the "large polaron" mobility have been summarized<sup>14</sup> and within a factor of 2 or so predict the magnitude of the measured mobility in amorphous  $\text{SiO}_2$  ( $22 \pm 2 \text{ cm}^2/\text{V sec}$  at 300 K). All the theories have in common the dependence of the mobility on the inverse of the Fröhlich polaron coupling constant  $\alpha$  and the temperature dependence of the population of the longitudinal optical (LO) mode.<sup>14</sup> In both  $\text{SiO}_2$  and  $\text{Al}_2\text{O}_3$  there are several LO modes, which in the

TABLE II. Characteristics of the four electron traps identified in the transient conductivity experiments. Only trap "4" has been associated with a specific impurity, substitutional  $\text{Cr}^{3+}$ .  $k_n$  is the trapping rate which will be proportional to the concentration of the trap and will vary somewhat from sample to sample; data given are for sample 2.  $q_n$  is the release rate from the trap and it is not dependent on concentration, but is exponentially dependent on temperature with the activation energy  $\Delta E$ ; values quoted are for 300 K.  $[n]$  is the estimated concentration of the traps for sample 1, and  $R_n$  is the estimated trap radius from the data fit to a diffusional model.

Trap	$k_n$ (sec <sup>-1</sup> )	$q_n$ (sec <sup>-1</sup> )	$[n]$ (cm <sup>-3</sup> )	$R_n$ (cm)	$\Delta E$ (eV)
"1"	$4 \times 10^7$	543			~0.8
"2"	$4.6 \times 10^8$	4.6	$\sim 10^{15}$	$\sim 5 \times 10^{-7}$	0.75
"3"	$1.5 \times 10^7$	$< 10^{-10}$	$\sim 2 \times 10^{15}$	$\sim 5 \times 10^{-9}$	~1.5 eV <sup>b</sup>
"4", $\text{Cr}^{3+}$	$4.6 \times 10^6$	$< 10^{-10}$	$\sim 3 \times 10^{16}$ <sup>a</sup>	$8 \times 10^{-11}$	>1.5 eV <sup>c</sup>

<sup>a</sup> Undoped sample.

<sup>b</sup> Annealing data.

<sup>c</sup> Reference 2.

first approximation can be summed to get the impedance (or inverse of the mobility). This approach, used by Lynch,<sup>15</sup> was successful for SiO<sub>2</sub>, so I will base the prediction for Al<sub>2</sub>O<sub>3</sub> on just the ratio of the differences with SiO<sub>2</sub>. The biggest difference is the much larger static dielectric constant in Al<sub>2</sub>O<sub>3</sub>, 9–11 depending on orientation compared with 4 for SiO<sub>2</sub>. The Fröhlich coupling constant can be calculated for each LO mode with the knowledge of the dielectric function for the material in the region of the mode energies. The dielectric function has been carefully determined for sapphire<sup>13</sup> and it is found that the strongest coupling is for the mode around 0.06 eV, which is also low enough in energy to be fairly well populated at 300 K. This is very close to the same dominant mode energy in SiO<sub>2</sub> and the ratio of polaron coupling constants is roughly  $2.7(\text{Al}_2\text{O}_3)/1.3(\text{SiO}_2) = 2$ . Thus the predicted mobility is about 15 cm<sup>2</sup>/V sec, which is more than a factor of 2 higher than is found. Even more disturbing than the low measured mobility is the lack of strong temperature dependence, which should be proportional to  $\exp(0.06 \text{ eV}/kT)$ . One of the reasons I pursued an investigation of pure sapphire was to compare it with the results I had obtained earlier on single-crystal quartz. In contrast to the high-purity Supracil 2 (amorphous SiO<sub>2</sub>), which showed the high mobility and the proper temperature dependence, the quartz crystals available to me, both synthetic and natural, displayed lower mobilities, about 5 cm<sup>2</sup>/V sec, and the same lack of temperature dependence that I report here for sapphire. It was hoped that the high purity of the sapphire (quartz cannot be grown by the Czochralski technique because of a phase change) would lead to the predicted high mobilities, at least at lower temperatures. As seen in Fig. 4, a mobility of 500, which would be expected from the large polaron theory, is not found.

At present I do not have a good explanation for these results. The lack of temperature dependence over a wide range presents great difficulties for any theory of the mobility; the problem is similar to that in the molecular crystals and the difficulties have been reviewed by Schein.<sup>16</sup> Impurity scattering can give essentially temperature-independent energy loss which adds to that due to phonon scattering, but to predict a mobility of 3 cm<sup>2</sup>/V sec there would have to be a scattering event in almost every unit cell and the defect concentration is obviously not that high.<sup>17</sup> There is the possibility of an impurity band which would maintain a temperature independence by virtue of the ground-state tunneling. Normally, impurity band transport in semiconductors occurs only at very low temperature because the impurity levels must be shallow to maintain

sufficient wavefunction overlap to give appreciable tunneling rates; at even 80 K the carrier transport occurs by fast thermal excitation out of the impurity level to the conduction band and the effect of the impurity is just additional scattering.<sup>18</sup> Thus the impurities would have to be very deep, but still have sufficient overlap for fast tunneling (rates of at least 10<sup>12</sup> hops/sec would be necessary). Also, the energy levels for an electron in the well would have to be separated in such a way that thermal excitation to levels higher in the well (with presumably faster tunneling rates) would be minimized even at 300 K. To my knowledge, a trapping site with these characteristics has escaped identification in other solids.

The mobility in the prompt pulse has not really been measured directly, as discussed in Sec. III D. At low temperatures the delayed sweepouts cannot be observed, so there is no actual measurement of the mobility—only the fact that both the mobility and lifetime are relatively unchanged. In a simple diffusional trapping model the trapping rate is related to the carrier mobility, the density of trapping sites  $N_n$ , and the trap radius  $R_n$  by

$$k_n = 4\pi\mu_p kT N_n R_n. \quad (16)$$

If  $\mu_p$  were really independent of temperature,  $\tau$  should increase by a factor of 3, which would be easy to observe and is not observed. If trap "2" is coulombic, then  $R_n \propto T^{-1}$ , and  $\mu\tau$  can be independent of temperature. From the same formula one predicts that the concentration of these positively charged traps is about 10<sup>15</sup> cm<sup>-3</sup> for a  $R_2$  of  $5 \times 10^{-7}$  cm (at 300 K).

## 2. "Trap-modulated" mobility

The time-of-flight mobility reported in Table I is trap modulated in the sense that the transport still takes place as in the prompt portion but that the electron spends most of its time in trap "2". In this case, the measured mobility is

$$\mu_{\text{eff}} \cong \mu_p q_2/k_2, \quad (17)$$

and the  $\mu_{\text{eff}}$  variations from sample to sample are mostly due to variations in  $k_2$ , which should be proportional to the concentration of trap "2". Although the structure of trap "2" is not yet known, it is not unlikely that its concentration would be different even in different cuts from the same boule since concentration gradients have been found for other impurities, most notably Cr<sup>3+</sup>.<sup>19</sup> Since the  $\mu_p$  are so difficult to measure in the samples where  $\tau$  is less than about  $2 \times 10^{-9}$ , it cannot be said for certain that there is an angular variation in  $\mu_p$  as might be assumed from the first glance at Table I. It seems fairly certain that the

anisotropy is not greater than about a factor of 2 in the three directions.

Some care must be exercised in obtaining  $\mu_{\text{eff}}$  from time-of-flight data. The transit time must be kept more than the inverse of the release rate,  $1/q_2$ , or else the transit time will not be inversely proportional to the applied field. The mobilities reported here were for transit times of 8 sec or more, while  $1/q_2$  is 0.2 sec.

The release rate  $q_2$  has an activation energy of 0.75 eV, which is the shallowest trap in this type of sapphire and has not been observed in previous TSC or TSL experiments. It is somewhat puzzling that  $q_1$  has close to the same activation energy, which means that as an electron trap its preexponential must be about 100 times larger than that of  $q_2$ . The significance of this is not understood at present.

#### C. $\text{Cr}^{3+}$ electron trap

It has been suspected that substitutional  $\text{Cr}^{3+}$  is an electron trap in sapphire.<sup>1</sup> Solid proof of this is given in Fig. 6, where increased deep trapping of the electrons is caused by the presence of  $\text{Cr}^{3+}$ . The marked nonlinearity of the lifetime on  $\text{Cr}^{3+}$  concentration can be understood in terms of the trapping model. The  $k_4$  is defined in terms of the  $\text{Cr}^{3+}$  concentration:  $k_4 = S[\text{Cr}^{3+}]$ , where  $S$  is a constant, and  $\tau_3$  now becomes

$$\tau_3 \cong \frac{k_2 + k_3 + S[\text{Cr}^{3+}]}{q_2(k_3 + S[\text{Cr}^{3+}])} \quad (10c)$$

The solid line in Fig. 6 is a fit to the data of Eq. (10c) with  $k_2 = 4.3 \times 10^8 \text{ sec}^{-1}$ ,  $k_3 = 1.5 \times 10^7 \text{ sec}^{-1}$ , and  $S = 8 \times 10^{-11}$ . As the  $\text{Cr}^{3+}$  concentration gets large it can be seen from Eq. (10c) that the lifetime asymptotically approaches  $1/q_2$ , and will become independent of the  $\text{Cr}^{3+}$  concentration. Of course, the prompt lifetime will continue to depend on  $[\text{Cr}^{3+}]$  as more electrons find it rather than trap "2". From Eq. (16) the  $R_4$  for the substitutional  $\text{Cr}^{3+}$  trap can be estimated as  $R_4 = 8 \times 10^{-11} \text{ cm}$ , which is quite a small trap radius even for a neutral trap.

#### D. Increased lifetime from trap filling

The reversible change in  $\tau_3$  with accumulated dose can be understood with an extension of the trap model to account for the filling of trap "3" by an accumulation of electron-hole pairs. At room temperature there is no significant emptying of an occupied trap. The data of Fig. 5 can be fit by assuming that  $k_3$  goes from  $1.5 \times 10^7 \text{ sec}^{-1}$  to 0 as trap "3" is filled and that  $k_4$  remains constant at  $4.6 \times 10^6 \text{ sec}^{-1}$ . The value for  $k_4$  implies a  $\text{Cr}^{3+}$  concentration of  $6 \times 10^{16} \text{ cm}^{-3}$  (about 1 ppm) which is close to the value found for "pure" Union Carbide

sapphire by neutron activation techniques.<sup>3</sup> The prediction of the shape of the lifetime as a function of accumulated dose is more complicated and can be obtained by a solution to the differential equation for  $k_3$  which is proportional to the concentration of unfilled trap "3" sites,  $n_3^0 - n_3$ , where  $n_3^0$  is the concentration in the virgin sample. In the steady-state approximation, with the dose rate constant and low enough to preclude bulk electron-hole recombination, the transcendental function for  $n_3^0 - n_3 = x$  is

$$Ax/k_4 + \ln x = -(GA/k_4)t + An_3^0/k_4 + \ln n_3^0, \quad (18)$$

where  $k_3 = Ax$ ,  $G$  is the rate of production of electron-hole pairs, and  $t$  is the elapsed time of irradiation.  $Gt$  is the total concentration of electron-hole pairs. The solid line in Fig. 5 is for  $A = 5 \times 10^{-9} \text{ cm}^3/\text{sec}$ , and a yield of  $3 \times 10^{12}$  (electron-hole pairs)/ $\text{cm}^3 \text{ rad}$ . The  $n_3^0$  turns out to be about  $2 \times 10^{15} \text{ cm}^{-3}$ , which is more than an order of magnitude lower than the  $\text{Cr}^{3+}$  concentration. The same model makes it clear why the lifetime in the doped  $\text{Cr}^{3+}$  samples cannot be significantly altered by accumulated irradiation. The  $\tau_3$  is so dominated by  $k_4$  that the predicted increase in  $\tau_3$  is only from 1.17 to 1.35 sec, which is inside the experimental error.

An interesting implication of the trap-filling experiment is that there is probably a roughly equal number of positively and negatively charged traps (with trap "3" being the positively charged ones). The reason for this conclusion is taken from the data on  $\text{SiO}_2$ , where a similar experiment leads to shorter electron lifetimes.<sup>7,20</sup> Careful experiments show that both electron and hole traps in pure  $\text{SiO}_2$  (thermally grown on Si) are neutral, so that as the trapped-hole population builds up, the electron lifetime is reduced by the high trap radius (measured to be a coulomb radius) positively charged sites where the holes are trapped. Thus I speculate that the same situation is avoided in sapphire by having roughly equal numbers of oppositely charged traps. The radius of trap "3" is found to be, in the diffusional approximation,  $5 \times 10^{-9} \text{ cm}$ , which is 60 times bigger than for the neutral  $\text{Cr}^{3+}$  trap. However, it is about a factor of 100 smaller than would be expected for a simple coulomb trap, like the trapped holes in amorphous  $\text{SiO}_2$ .

An attempt was made to change the value of  $k_1$  and/or  $k_2$  by irradiating the sample at 100°K, checking the  $k_1 + k_2$  rate without warming the sample. No significant change was found up to  $10^9$  rad accumulated dose.

#### V. SUMMARY AND CONCLUSIONS

In the study of color centers the dynamics of the electrons and holes in the original formation of the

color center are usually not known. This paper gives the kinetics of the diffusion of the "free" electron and the trapping and detrapping parameters for four separate electron traps. Kinetic information gives characteristics of the traps which are not available by other techniques, such as the very fast trapping and detrapping rates, the number of traps (from trap filling and doping of  $\text{Cr}^{3+}$ ), and the trapping radii. Lee and Crawford<sup>1</sup> have pointed out that in sapphire much more is known about hole traps (from EPR and optical studies) than about the electron traps. I have been able to separate the  $\text{Cr}^{3+}$  trap (which was suspected previously of being an electron trap) from three other electron traps which are present. Traps "1" and "2" will not stay populated at room temperature but if the samples were irradiated and maintained at low temperature their EPR or optical properties might allow a determination of their nature.

There are many possible lattice defects and impurities which might be trap "3". One possibility would be the  $\text{Ti}^{4+}$  substitutional, which has a net positive charge. Cox<sup>21</sup> has studied crystals which have been doped with equal amounts of Mg and Ti and finds that they go in substitutionally as  $\text{Mg}^{2+}$  and  $\text{Ti}^{4+}$  centers which charge compensate each other. When the doped crystals are x rayed, the holes are trapped at the Mg site and are well characterized by ESR. Cox assumes that the electrons are trapped at the Ti site but does not provide optical or ESR evidence for this. The ESR spectrum of holes trapped at Mg sites have not been reported in the pure Czochralski grown crystals, but analysis<sup>3</sup> confirms the presence of Mg in a concentration of a few ppm, and Ti in concentrations of less than 3 ppm.

In this model of the trap-filling effect, a hole trapped at a  $\text{Mg}^{2+}$  site must have a smaller trapping radius for electrons (by more than an order of magnitude) than the original  $\text{Ti}^{4+}$  site. In the simple Coulomb trapping model this means that the charge compensating sites must not be too close together. For each to act independently as coulomb trapping sites for electrons or holes they must be more than 50 Å apart (at 300°K). The data show that the trapping radius is less than that for a simple Coulomb center and this may be due to the proximity, on the average, of the charge compensating sites. Of course, this simple model only considers two kinds of traps, coulomb attractive with a large radius (about  $5 \times 10^{-7}$  cm at 300 K), and neutral geometric traps which are neither attractive or repulsive and thus in a random-walk model have trap radii of  $\sim 10^{-8}$  cm. Deep traps with trap radii much smaller than  $10^{-8}$  cm (like the  $\text{Cr}^{3+}$  trap reported here) are common in the semiconductor literature,<sup>18</sup> and the reasons for the

repulsive lip on the trap are not usually understood. Thus I do not believe it is possible to predict whether an electron trap like  $\text{Ti}^{4+}$  has a larger radius than a trapped hole at a  $\text{Mg}^{2+}$  except on the simple Coulomb model. Predictions of a repulsive lip on a trap will involve detailed knowledge of the trapping dynamics (for example, polaron effects).

Trap filling which leads to an increased lifetime for a species as I have shown for trap "3" is a little observed but potentially important phenomenon. Such trap filling has been proposed as a vital part of the switching mechanism in amorphous semiconductors, where the low mobilities measured in drift experiments give way to mobilities (and consequently currents) many orders of magnitude higher if the traps can be filled on a transient basis.<sup>22</sup> This will not work with neutral traps or traps of only one sign because of space charge and trap radius problems, described above. Thus the occurrence of charged traps of both signs and roughly equal numbers becomes a necessity in the switching model; a model of charge compensating defects is a plausible explanation.

An important issue in the discussion of transport in  $\text{SiO}_2$  has been the formation of small polarons by holes. The electrons in  $\text{SiO}_2$  exhibit the high, "large" polaron mobility with lifetimes which seem dominated by defect trapping rather than small polaron formation with nanosecond delay times. The holes, on the other hand, are low mobility from very early time, and evidence has been presented by Hughes and Emin<sup>23</sup> that the holes indeed form small polarons. In sapphire, I have not been able to distinguish the hole transport in the presence of the dominating electron transport. Several kinds of hole traps have been identified, and their concentration is in the 1-ppm-or-less range. Thus, even though one might expect that holes would form small polarons in  $\text{Al}_2\text{O}_3$  in analogy to  $\text{SiO}_2$ , I cannot present any definitive evidence from the data presented here one way or the other. It is clear from the data that the overall mobility-lifetime product is much greater for electrons than holes. Net positive charging of the silicon sapphire interfacial region has been noted in irradiated silicon-on-sapphire (SOS) integrated circuits and is consistent with the present results.<sup>24</sup>

#### ACKNOWLEDGMENTS

I would like to thank Roger Klafky of BNL for technical discussions and the  $\text{Cr}^{3+}$ -doped samples, Zoltan Soos for help with the analysis, George Arnold for discussions of radiation damage in  $\text{Al}_2\text{O}_3$ , and David Evans for technical assistance. This work was supported by the U. S. Department of Energy under Contract AT (29-1)-789.

- \*A U. S. Dept. of Energy Facility.
- <sup>1</sup>K. H. Lee and J. H. Crawford, Jr., *Phys. Rev. B* **15**, 4065 (1977).
- <sup>2</sup>K. H. Lee, G. E. Holmberg, and J. H. Crawford, Jr., *Phys. Status Solidi A* **39**, 669 (1977).
- <sup>3</sup>C. F. Bauer and D. H. Whitmore, *J. Solid State Chem.* **11**, 38 (1974); B. D. Evans and M. Stapelbroek, *Phys. Rev. B* **18**, 7089 (1978).
- <sup>4</sup>R. C. Hughes, *J. Chem. Phys.* **55**, 5442 (1971).
- <sup>5</sup>R. C. Hughes, *Radiat. Eff.* **26**, 225 (1975).
- <sup>6</sup>W. L. Chadsey, J. C. Garth, R. L. Sheppard, and R. Murphy, X-ray Dose Enhancement (unpublished), Vol. 1; Summary Report, Report No. RADC-TR-76-159, Defense Nuclear Agency (unpublished). Available through NTIS.
- <sup>7</sup>R. C. Hughes, *Solid State Electron.* **21**, 251 (1978).
- <sup>8</sup>R. C. Hughes, E. P. EerNisse, and H. J. Stein, *IEEE Trans. Nucl. Sci.* **22**, 2229 (1975).
- <sup>9</sup>R. C. Hughes, *Phys. Rev. Lett.* **35**, 449 (1975).
- <sup>10</sup>K. K. Thornber and R. P. Feynman, *Phys. Rev. B* **1**, 4099 (1970).
- <sup>11</sup>K. K. Thornber, *Solid State Electron.* **21**, 259 (1978).
- <sup>12</sup>D. K. Ferry in *The Physics of SiO<sub>2</sub> and Its Interfaces*, edited by S. T. Pantelides (Pergamon, New York, 1978), p. 29.
- <sup>13</sup>A. S. Barker, Jr., *Phys. Rev.* **132**, 1474 (1963).
- <sup>14</sup>J. J. O'Dwyer, *The Theory of Electrical Conductors and Breakdown in Solid Dielectrics* (Clarendon, Oxford, 1973), Chap. 2.
- <sup>15</sup>W. T. Lynch, *J. Appl. Phys.* **43**, 3274 (1972).
- <sup>16</sup>L. B. Schein, *Phys. Rev. B* **15**, 1024 (1977).
- <sup>17</sup>L. B. Schein, C. B. Duke, and A. R. McGhie, *Phys. Rev. Lett.* **40**, 197 (1978).
- <sup>18</sup>A. G. Milnes, *Deep Impurities in Semiconductors* (Wiley-Interscience, New York, 1973).
- <sup>19</sup>F. R. Charvat, J. C. Smith, and O. H. Nestor, in *Crystal Growth*, edited by H. S. Pieser (Pergamon, New York, 1967), p. 45.
- <sup>20</sup>W. C. Johnson, Study of Electron Transport and Breakdown in Thin Insulating Films, Report No. NVL-0059-003 (1976) (unpublished).
- <sup>21</sup>R. T. Cox, *Solid State Commun.* **9**, 1989 (1971).
- <sup>22</sup>K. Subhani, M. S. Shur, M. P. Shaw, and D. Adler, in *Proceedings of the Seventh International Conference on Amorphous and Liquid Semiconductors*, edited by W. E. Spear (University of Edinburgh, Edinburgh, 1977), p. 712.
- <sup>23</sup>R. C. Hughes and D. Emin, in *The Physics of SiO<sub>2</sub>*, edited by S. T. Pantelides (Pergamon, New York, 1978), p. 14.
- <sup>24</sup>J. R. Srour, S. Othmer, and S. C. Chen, *IEEE Trans. Nucl. Sci.* **24**, 2119 (1977).